JOURNAL OF CATALYSIS 18, 200–211 (1970)

Surface Reactivity of Supported Gold

I. Oxygen Transfer Between CO and CO_2

D. Y. CHA* AND G. PARRAVANO

Department of Chemical and Metallurgical Engineering, The University of Michigan, Ann Arbor, Michigan 48104

Received October 24, 1969

The rate of redistribution of isotopic carbon between CO and CO_2 has been studied on Au supported on MgO in the temperature range 300 to 400°C, P_{CO_2}/P_{CO} ratios 0.1 to 1.2 and total pressure of 50 Torr. A few experiments were also carried out on supported Ru and Pt. The effect of Au concentration, temperature, and catalyst preparation method have been selected for investigation. In addition, determinations of the particle size of Au have been carried out by X-ray to illustrate the effect of the temperature of reduction and decomposition of the Au salt upon the particle size of the metal in the supported catalyst. Chemical reduction of the Au salt at low temperature (<100°C) produced Au particles with diameters ≤150 Å, while particles with diameters 20 times larger were obtained by thermal decomposition (≤350°C) of the Au salt. Since particle growth may occur by direct addition of the decomposing salt and/or by sintering among metal particles, it is suggested that the latter process cannot readily occur at temperatures ≤0.3 Tm. The implications of these findings for separate control of the degree of dispersion and of the support coverage by the metal are pointed out.

Kinetic observations have been employed to study the thermodynamic and kinetic factors contributing to the activity of Au surfaces in the oxygen transfer step between gas and surface phases. Au activity was found to decrease with increasing P_{CO_2}/P_{CO} ratio, indicating that reduced surface species (metal atoms) play a dominant role in the reactivity of the surface. A similar trend was found for Ru and Pt at low ratios P_{CO_2}/P_{CO}. For Pt at higher P_{CO_2}/P_{CO} ratios, a reactivity inversion was found. Under similar conditions of gas composition, temperature and support, the affinity of the Au surface for oxygen increased with decreasing particle size. The degree of dispersion of Au was found to influence the rate of the catalytic reaction. The effect has been interpreted in terms of a relation between metal particle size and gas mean free path.

The usefulness of these studies for developing criteria for control of oxidation depth and selectivity behavior in catalytic oxidations through optimization of size, size distribution of metal particles, and their morphological connection with the supporting agent is emphasized.

The enhancement of surface reactivity of metals through dispersion into a finely divided form is a well-known effect. The chemical inertness of bulk or massive Au is a unique property among all metals. This fact suggests that Au should be an interesting metal for investigating the dispersion effect since studies on the chemical reactivity of finely divided Au may bring out surface behavior in a more striking and direct fashion than it is possible to obtain with other metals, thus providing information on the role of physical and/or chemical factors in surface reactivity of metals, including particle size, particle size distribution and influence of support and additions.

Among the molecular interactions at Au

* Present address: The Upjohn Company, Kalamazoo, Michigan.

surfaces that may be considered for studies on the reactivity enhancement by dispersion none seems more relevant than that involving species containing oxygen. In fact, there is conflicting evidence on the adsorption of oxygen on Au (*1*). Generally, contact potential measurements indicated an interaction between Au films and atomic (*2*) or molecular (*3*) oxygen. However, no information is available on the affinity of Au for oxygen derived from oxygen donor molecules other than molecular O_2. Therefore investigations on the extent to which dispersion of Au into a solid matrix modifies the metal reactivity towards oxygen are of special importance.

To appraise simultaneously the thermodynamic and kinetic aspects of the surface reactivity of Au, it is necessary to investigate the rate of a surface reaction at equilibrium. This is conveniently carried out by employing an isotopic exchange reaction. Redistribution of a carbon tracer between CO and CO_2 was the reaction chosen in this work, namely:

$$^*CO_2(g) + CO(g) \rightarrow CO_2(g) + {}^*CO(g). \quad (1)$$

Reaction (1) may be considered the sequence of two reaction steps of equal velocity since they represent the forward and reverse steps of a chemical equilibrium, namely:

$$^*CO_2(g) \rightarrow {}^*CO(g) + O(s), \quad (1a)$$
$$CO(g) + O(s) \rightarrow CO_2(g). \quad (1b)$$

Therefore, the rate of reaction (1) gives directly the rate of reactions (1a), (1b), which represents the elementary transfer steps, characterizing the Au–oxygen interaction at the surface. Reaction (1) has already been employed to investigate oxygen transfer at the surface of metal oxides (*4*) and metals (*5*). The latter study was carried out in the temperature range 800–1000°C on metal foils.

The experimental results of the present research were gathered on Au preparations supported on MgO and Al_2O_3 with varying Au content, 0.3 to 5 wt %, temperatures of 300 to 400°C and ratios p_{CO_2}/p_{CO} 0.1 to 1.2. To compare the behavior of finely divided Au with that of transition metals a few experiments on supported Pt and Ru were also performed and are reported below.

Experimental Methods

Materials

Catalytic supports tested include: MgO, Al_2O_3, TiO_2, La_2O_3, and CeO_2. Only MgO was found to produce catalysts with sufficient activity for quantitative kinetic studies.

Two methods for the preparation of supported Au were employed. In one, a desired amount of $HAuCl_4 \cdot 3H_2O$ (reagent grade) was dissolved in distilled H_2O. To the solution, made slightly acidic with HCl, a weighed amount of MgO (reagent grade) was added at room temperature, and, subsequently, a 3% oxalic acid solution. The suspension was heated in a water bath for 2 hr. The mixture was cooled and washed several times with distilled H_2O, dried in air, and heated at 350°C for 2 hrs at 0.1 Torr.

Au catalysts were also prepared by impregnation of the support with H_2O solution of $HAuCl_4 \cdot 3H_2O$, in sufficient amount to produce a paste of creamy consistence. The paste was dried in air and heat treated at 350°C, similarly to the previous preparation. Pt and Ru supported catalysts were prepared by impregnation of high area (200 m^2/g) powdered Al_2O_3 with H_2O solutions of $PtCl_3$ and $Ru(NO)(NO_2)_3$ to give a final composition of ~1 wt % of metal. The subsequent heat treatment was similar to that employed for Au catalysts.

The particle size of supported Au was measured by the X-ray peak broadening method and reduced according to Jones' method (*6*). MgO was used as the standard to determine the instrument factor. The peaks for the samples containing 0.3, 0.7, and 2 wt % Au were small for accurate determination of the half peak width. The error limit of ±20 Å was assigned for these samples on the basis that the half peak width was between 2 and 4°. The error limit for the other samples is estimated to be about ±10%.

The catalyst containing 5 wt % Au on

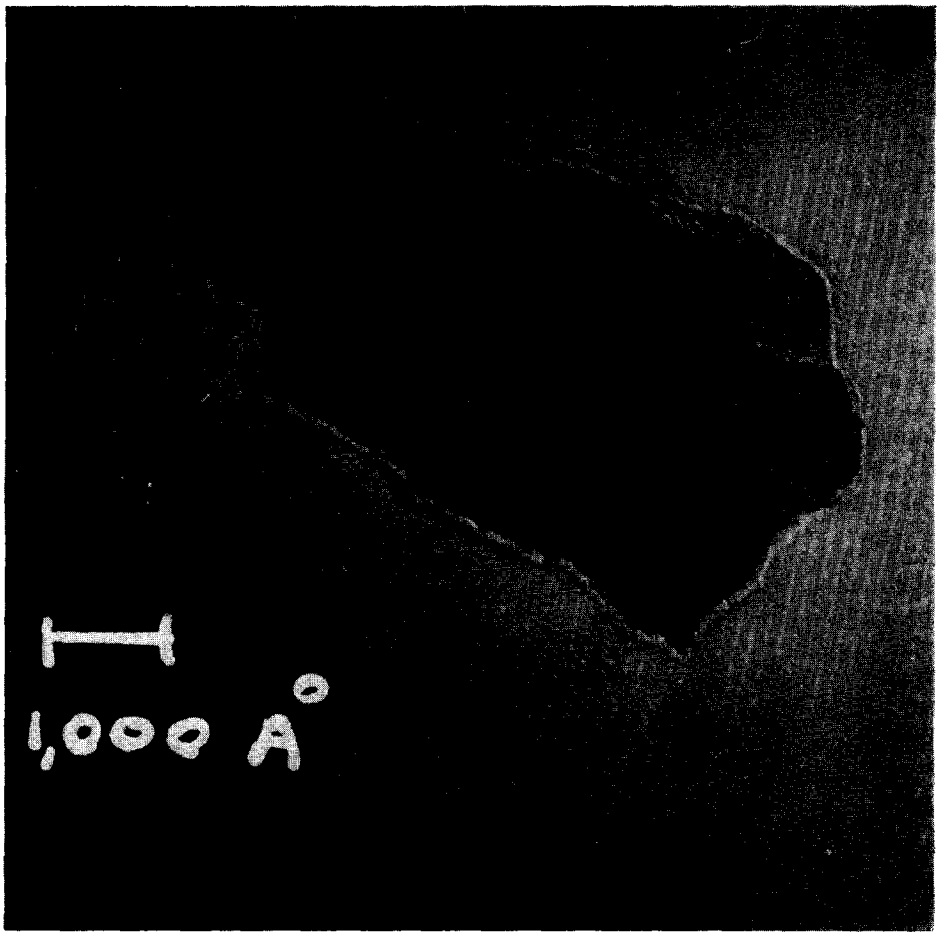

FIG. 1. Electron micrograph of Au (5 wt %)–MgO.

MgO and prepared by chemical reduction was observed under the electron microscope. It showed spherical gold particles not much imbedded into the matrix (Fig. 1). This is consistent with previous findings (7). The statistical distribution of particle diameters, obtained from these pictures (Fig. 2), yielded an average diameter of ~140 Å,

TABLE 1

CHARACTERISTICS OF Au–MgO CATALYSTS: PARTICLE DIAMETER, d; NUMBER OF PARTICLES PER GRAM OF METAL, n; SPECIFIC SURFACE AREA A, AND COVERAGE OF SUPPORT, D

Catalyst method of preparation	Au (wt %)	d (Å)	n (g^{-1})	A ($m^2\ g^{-1}$)	D^a (%)
Precipitation	0.3	40 ± 20	2.37×10^{15}	0.186	1.02
Precipitation	0.7	50 ± 20	5.14×10^{15}	0.435	2.39
Decomposition	0.7	1321 ± 130	3.01×10^{11}	0.0165	0.091
Precipitation	2.0	50 ± 20	1.58×10^{16}	1.242	6.83
Decomposition	2.0	1050 ± 130	1.70×10^{12}	0.0582	0.32
Precipitation	5.0	150 ± 13	1.46×10^{15}	1.035	5.69

[a] Calculated assuming a monoatomic film of Au on MgO.

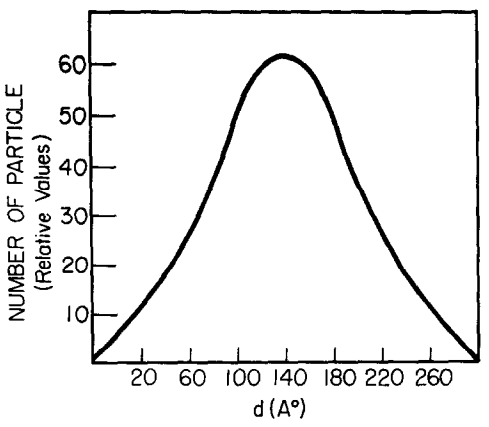

FIG. 2. Frequency distribution of Au particle diameters, d, for Au(wt %)–MgO by electron microscopy.

in good agreement with the value of 150 Å obtained from X-ray measurements.

From the latter results, the number of spherical Au particles, n, and their area per gram of metal, A, were calculated (Table 1). The MgO support was found to have a BET surface area of 18 $m^2\ g^{-1}$.

Apparatus and Procedure

The rate of reaction (1) was studied in an all glass, static system, consisting of gas purification, mixing and storage trains, reactor, and high vacuum line. A Geiger counter was used for the measurement of radioactive components in the gas mixture. CO and CO_2, from commercial cylinders, were introduced into storage bulbs after passage through Drierite. Mass spectrometric analysis showed only traces of oxygen present in the gases. $^*CO_2$, in sealed glass ampules, was transferred and mixed with $CO + CO_2$ mixtures. Several of these were prepared and stored in glass bulbs to provide mixtures with different p_{CO_2}/p_{CO} ratios. A weighed amount of catalyst (0.5 to 2 g) was placed in a ceramic boat and loaded in the reactor of 507 ml. Before introducing the $CO_2 + CO + {}^*CO_2$ mixture, each sample was outgassed at 400°C and 10^{-4} Torr for 24 hr. Gas samples (~25 ml) were withdrawn from the reactor at various time intervals with the aid of a Toepler pump and introduced into a glass cell, whose side was sealed with a mica window against which the Geiger counter was positioned. The total $^*CO_2 + {}^*CO$ count was recorded.

The gas was then pumped several times through a trap, kept at liquid N_2 temperature, to condense $^*CO_2 + CO_2$. The noncondensable gas was counted again to give the amount of *CO present. After analysis, CO and CO_2 were reintroduced into the reactor. The total pressure varied between 20 to 50 Torr. Radioactive counts were corrected for background statistical fluctuations. The possibility of the presence of side reactions, particularly CO disproportionation, was investigated and found negligible. No corrections for side reactions were, therefore, employed in the treatment of the experimental results.

A more detailed discussion on the preparation of catalysts and experimental procedure employed is recorded elsewhere (*8*).

EXPERIMENTAL RESULTS

Various catalyst preparations were screened for sufficient activity for quantitative results. A summary of these tests is reported in Table 2. The tests indicated

TABLE 2

CATALYTIC ACTIVITY OF SUPPORTED Au FOR REACTION (1), 350°C, (p_{CO_2}/p_{CO}) ≈ 1, TOTAL PRESSURE 50 TORR

Catalysts			
Support	Preparation	Au (wt %)	Relative activity
Al_2O_3	Precipitation	0.7	Weak
		5.0	Weak
Al_2O_3	Decomposition	5.0	Weak
MgO	Precipitation	0.3	Strong
		0.7	Strong
		2.0	Very strong
		5.0	Strong
MgO	Decomposition	0.7	Weak
		2.0	Weak
TiO_2	Decomposition	0.7	Very weak
La_2O_3	Decomposition	0.7	Very weak
Ce_2O_3	Reduction of $AuCl_3$ with Ce-oxalate and decomposition	0.7	No activity

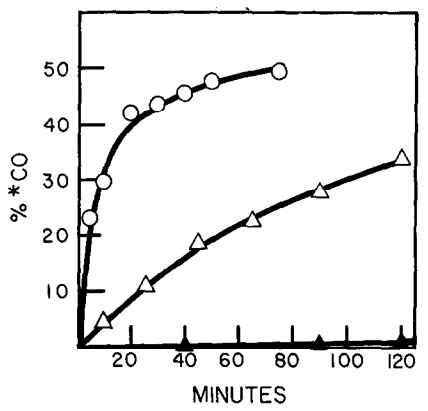

FIG. 3. Comparison of catalytic activity of Au–MgO preparations for reaction (1): ○, 2 wt %, 1, g. precipitation; ▲, 0.7 wt %, 1.85 g, precipitation; △, 0.7 wt %, 1.85 g, impregnation, 350°C, β = 0.78,

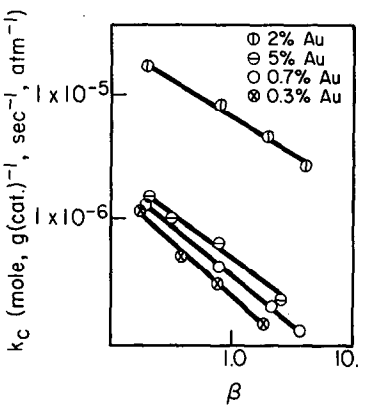

FIG. 5. Rate coefficient for reaction (1), k_c, catalyzed by Au–MgO preparations obtained by precipitation as a function of β; 350°C. Au content (wt %): ⊕, 2; ⊖, 5; ○, 0.7; ⊗, 0.3.

that MgO was a superior support. However, large differences among catalysts supported on MgO were found depending upon the procedure employed in the preparation of the catalyst.

Catalysts prepared by low temperature precipitation were found to be more active than those obtained by high temperature decomposition (Fig. 3). As a consequence, it was decided to perform quantitative rate studies on the Au–MgO preparations obtained by low temperature precipitation.

In Figure 4, typical results on Au (0.3 wt %)–MgO obtained at 350°C and different ratios (p_{CO_2}/p_{CO}) = β are reported. Similar curves were obtained with catalysts containing different concentrations of Au. No catalytic activity could be detected on pure MgO and Al_2O_3 at 350°C. From the initial slopes of the plots of the time dependence of [*CO], the rate coefficient, k_c, for reaction (1) was computed by means of the expression:

$$k_c = \frac{\text{initial slope} \times V_R}{W \times T_R \times R},$$

where V_R, T_R, and W are the volume and temperature of the reactor and catalyst weight, respectively, and R the gas constant. The experimental dependence of k_c upon β is shown in Fig. 5, for Au, while

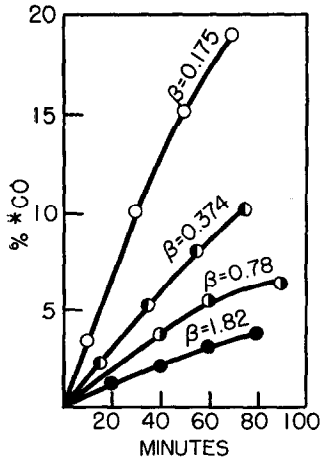

FIG. 4. Formation of *CO according to reaction (1) catalyzed by Au(0.3 wt %)–MgO, 1 g, precipitation, 350°C; β: 0.175 ○; 0.374 ◐; 0.78 ◑; 1.82 ●.

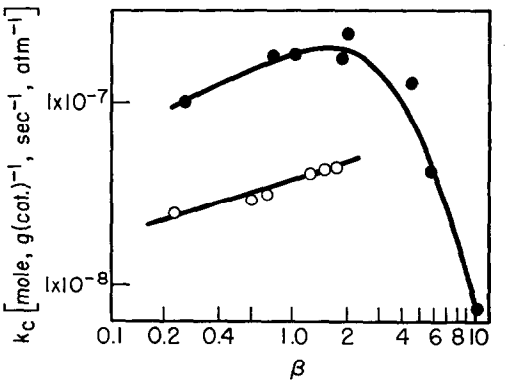

FIG. 6. Rate coefficient, k_c for reaction (1) catalyzed by Pt(1 wt %)–Al_2O_3 as a function of β: ○, 356°C; ●, 405°C.

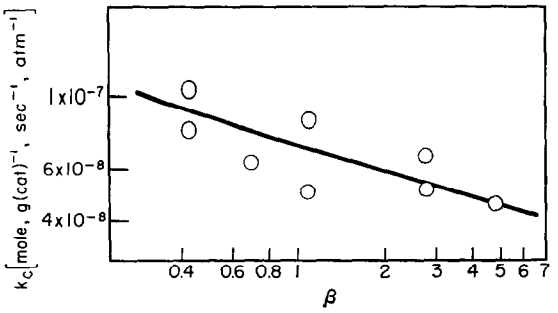

FIG. 7. Rate coefficient, k_c, for reaction (1) catalyzed by Ru (1 wt %)–Al_2O_3 as a function of β, 350°C.

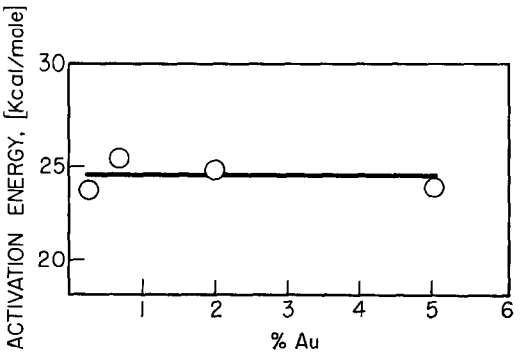

FIG. 8. Activation energy for reaction (1) catalyzed by Au–MgO, obtained by precipitation as a function of the wt % of Au $\beta = 0.78$, 300–375°C.

the results on Pt–Al_2O_3 and Ru–Al_2O_3 in the temperature interval 350–405°C are shown in Figs. 6 and 7, respectively. The slopes of the straight lines drawn through the experimental points are collected in Table 3.

TABLE 3

VALUE OF THE SLOPE, m, OF PLOTS OF k_c VS β FOR REACTION (1) CATALYZED BY SUPPORTED Au, Pt, AND Ru

Metal	Amount (wt %)	Support	Temp (°C)	m
Au	0.3	MgO	350	−0.8
Au	0.7	MgO	350	−0.7
Au	2.0	MgO	350	−0.6
Au	5.0	MgO	350	−0.7
Pt	1.0	Al_2O_3	356	0.3
Pt	1.0	Al_2O_3	405	0.4 ($\beta > 2$)
			405	−3.0 ($\beta < 2$)
Ru	1.0	Al_2O_3	350	−0.3

In the range 300–375°C and $\beta = 0.78$, the activation energy for the Au catalysts was found to be 23.6 to 25.5 kcal/mole for Au and 27.0 kcal/mole for Pt. The activation energy was not dependent upon the Au content of the catalyst (Fig. 8).

DISCUSSION

Catalyst Characterization

Table 1 shows that Au preparations, obtained by low temperature precipitation of the Au salt, produced smaller Au particles than the preparations obtained by high temperature decomposition of the Au salt. The difference in particle size—by a factor of about 20–25—is quite striking, indicating that a radically different mechanism for the growth of the Au particles was operative in the two cases. It appears that the growth of metal particles can occur at reasonable rates of 350°C only through direct grain growth and not through intraparticle sintering. At high temperature after the initial formation of some metal nuclei, their growth rate is relatively fast in relation to the rate of new nuclei formation. This is the result of high ionic and atomic mobility and availability of undecomposed salt. Thus, the Au particles initially formed tend to grow by addition of decomposing Au salt. At low temperature, once particle formation has taken place by chemical reduction of the salt present and precipitation of the metal, the only manner for particles to grow is through intraparticle sintering. At 350°C or 0.25 Tm this cannot occur readily among supported Au particles. Here Tm is the Tamman temperature of Au. This interpretation is consistent with the observation of a not too broad size distribution for the low temperature preparation (Fig. 2). It must also be stressed that these conclusions apply to Au particles dispersed on a low area, highly crystalline support, like MgO, and cannot be directly extrapolated to morphologically different supports, (Al_2O_3). However, from the results of Table 1, it seems clear that control of particle size and size retention at operating temperatures may be conveniently obtained by low temperature precipitation of the metal salt on the support.

The influence of the support is essentially twofold. Firstly, it plays a role in the mechanism of decomposition of the salt by exerting an indirect (catalytic) and/or direct control of the path followed by the decomposition reaction. This may include the local concentration of decomposition products, the mobility of the metal ions, the formation of volatile species. These effects are important for the formation of the initial metal nuclei. Secondly, the support influences the rate and morphology of growth of the critical nuclei through its primary and secondary physical structure —its degree of cristallinity, apparent and bulk density.

Catalyst Activity

The significant experimental results, recorded in the previous section, on the catalytic activity of Au–MgO preparations for reaction (1) are:

1. High catalytic activity was obtained only with samples prepared by low temperature reduction of the Au salt.
2. The specific catalytic activity of Au varied with dispersion; the maximum activity corresponded to the catalyst containing 2 wt % of Au.
3. The experimental rate coefficient for reaction (1) k_c, was dependent upon β. For Au and Ru, k_c was found to decrease with increasing β, or $k_c = k\ \beta^{-m}$ (2) where k and m are constants and $0.6 \leq m \leq 0.8$.
4. For Pt–Al_2O_3 catalysts, a positive slope was found at 356°C. At 405°C, positive and negative slopes were obtained depending upon the value of β. Thus an inversion in surface reactivity took place.

These conclusions point to the fact that the onset of readily measurable activity for oxygen transfer between gas phase and Au surfaces is dependent upon the presence of Au particles of sufficiently small size ($\sim<100$ Å). This is consistent with the general nature of the dispersion effect. The low temperature procedure for the reduction of the Au salt is similar to the classical method employed for the preparation of metal sols. Essentially, through this procedure the formation of initially small Au particles, statistically and firmly deposited on the support at large intraparticle distances takes place. As suggested previously these conditions may be instrumental in inhibiting subsequent grain growth and sintering of the Au particles at higher temperature. There is also the likelihood that catalysts prepared by chemical reduction had a lower Cl content than those prepared by high temperature decomposition. However, a large influence of Cl upon oxygen transfer activity (not selectivity) of metal catalysts had not been reported before and seems unlikely. Recent investigations (*7*) by Mössbauer spectroscopy on chemical and morphological changes which $HAuCl_4$, impregnated an Al_2O_3 and MgO undergoes during its decomposition revealed the presence of an intermediate state of Au characterized by a lower electron density at the nucleus than that of Au metal. This may be the result of the presence of a strong electronegative environment. Conceivably this effect is related to the decomposition mechanism followed by the metal salt and, consequently, to the influence of the preparation procedure upon morphology and activity of Au, as found in the present work.

To probe into the origin of the influence of the size of Au particles upon the reactivity of their surface towards oxygen, an analysis of the thermodynamic and kinetic factors involved is carried out. The analytical treatment of the rate of reaction (1), previously discussed in detail (*3*), is based on the rate coefficient, k_c, defined by the rate expression for reaction (1):

$$-\frac{1}{W}\frac{dp_{CO_2}}{dt} = k_c p_{CO_2} - k'_c p_{*CO}, \qquad (2)$$

where k_c' is the rate coefficient of the reverse reaction. k_c is experimentally related to β by expression (2) through the reaction rate constant, k, and the exponent m.

Surface Stoichiometry

To interpret the experimentally observed values of m, a surface reaction equilibrium and a rate controlling step that underlie reaction (1) when catalyzed by a solid surface must be formulated. For the gas–sur-

face reaction equilibrium, which produces and destroys surface centers by reaction with the $CO + CO_2$ mixture, we shall assume the following:

$$CO_2(g) + xMe(s) \rightleftharpoons CO(g) + Me_xO(s). \quad (3)$$

In general fashion, the oxygen donor molecule from the gas phase may be bound at surface reduced sites $[Me(s)]$ or oxidized sites $[Me_xO(s)]$.

The experimental observation that the exponent m in Eq. (2) was found to be negative demonstrates that the concentration of the centers of surface activity decreased with increasing oxidation power of the gas phase. Thus, surface Au atoms had a more direct role in the adsorption of oxygen. In reaction (3) s indicates the number of surface atoms required for the adsorption of one oxygen atom. $Me(s)$ and $Me_xO(s)$ may be considered similar to surface defects: adsorbed cations (or interstitial cations) and oxygen vacancies, respectively. Assuming that the defective structure of the surface layer is such that $[Me(s)]$ $[(Me_xO(s)] = \text{const}$, the application of the mass action expression in simple form to surface equilibrium (3) yields:

$$[Me(s)] \propto \beta^{-[1/(1+x)]}.$$

The rate determining step for reaction (1) is written as:

$$*CO_2(g) + Au(s) \rightarrow *CO + AuO, \quad (4)$$

and its rate

$$\frac{dp_{*CO}}{dt} = k p_{*CO_2}[Au(s)]$$
$$= k\beta^{-[1/(1+x)]} p_{*CO_2} = k\beta^{-m} p_{*CO_2}. \quad (5)$$

Equation (5) reproduces the experimentally observed dependence between k_c and β.

The discussion on the reactivity of Au particles towards oxygen will then be centered upon reaction equilibrium (3) and rate determining step (4).

Tables 2 and 3 show that upon decreasing the Au particle diameter the oxidation equilibrium level of the Au surface increases; that is, under similar conditions of gas composition, temperature, and support, Au becomes less noble as its particle size decreases.

Intuitively, the result is expected. It shows that the thermodynamic affinity for oxygen can be influenced by the particle size of the metal. This is an important conclusion, particularly for the problem of oxidation depth and selective behavior in oxidation catalysis where a particular value of the surface oxygen affinity must be optimized. The analysis of the particle size effect points also to the fact that in the most active catalyst, Au–MgO, (2 wt %) surface Au atoms were in the least oxidation state, (formally Au_2O_3).

For Ru catalysts it was found $m = -0.3$ (Table 3), which indicates formal oxidation level of the surface of +4. For Pt catalysts, the results are more complex. At 356°C, $m = 0.3$. The positive value of m suggests a rate controlling step different from reaction step (4). Let us assume a rate controlling stage which includes the surface oxidized groups Me_xO:

$$*CO_2(g) + Me_xO(s) \rightarrow *CO(g) + Me_xO_2(s), \quad (6)$$

whose concentration is governed by equilibrium (3), or:

$$[Me_xO(s)] \propto \beta^{1/(1+x)}. \quad (7)$$

By means of expression (7), the rate of reaction (6) is now given by:

$$-\frac{dp_{CO_2}}{dt} = k p_{*CO_2}[Me_xO] = k p_{*CO}\beta^{1/(1+x)}. \quad (8)$$

For Pt it was found that the change in controlling step was brought about by temperature and β. At 405°C for $\beta > 2$, m was negative while for $\beta < 2$, it became positive (Fig. 7). The change of sign of m represents a true inversion in the reactivity pattern of the surface: for m positive, the rate reaction increases while it decreases for m negative with increasing oxidation power of the gas phase. Thus, for the range of conditions under which m is positive, the surface sites, active for oxygen transfer, increase with increasing partial pressure of the oxygen donor, contrary to what one would generally expect.

Despite the qualitative character of these

conclusions, they indicate the crucial role of the surface redox level in controlling the reactivity mechanism. In fact, reaction step (4), indicative of a less oxidized surface than reaction step (7), occurs at higher temperatures (405°C) than the latter (356°C). The influence of β is less clear. At low β, the surface is presumably largely bare, Me(s) sites are plentiful and the MeO(s) sites are controlling surface reactivity. Conversely, at high β. The implications behind the presence of a *maximum* instead of a *minimum* in the k_c vs β plot for Pt at 405°C are not clear.

Kinetic Effect

With the aid of Eq. (2), the values of the rate constant k were calculated for the various catalysts and are reported in Table 4. Generally, Pt is considered an overall oxidation catalyst superior to Ru and Au. However, the results of Table 4 show that the correct combination of support and preparation procedure may offset any effect of the intrinsic chemical nature of the catalytic material and increase the catalytic activity of Au up to four orders of magnitude higher than that of Pt. Any generalization and correlation of catalytic activity of metals not based on similar preparation procedure should be viewed with caution.

To assess whether specific surface effects

TABLE 4
RATE CONSTANT, k, FOR REACTION (1) CATALYZED BY SUPPORTED METALS[a]

Catalyst			
Metal	Metal (wt %)	Temp	k [mole g(cat)$^{-1}$ sec^{-1} atm^{-1}]
Au	0.3	350	2.5×10^{-7}
Au	0.7	350	3.6×10^{-7}
Au	2.0	350	6.8×10^{-6}
Au	5.0	350	4.9×10^{-7}
Pt	1.0	356	6.7×10^{-10}
Pt	1.0	405	3.1×10^{-9}
Ru	1.0	350	1.5×10^{-7}

[a] Au catalysts supported on MgO and prepared by reduction; Pt, Ru supported on Al_2O_3 and prepared by decomposition of the metal salt.

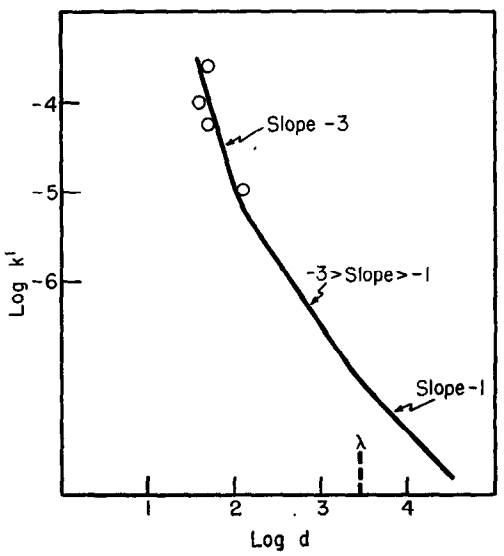

FIG. 9. Reaction rate constant per unit weight of Au, k', and particle diameter, d, 350°C, catalyst prepared by: low temperature reduction, high temperature decomposition. Theoretical slopes based on the model discussed in the text are also shown.

were present in the supported Au catalysts, the rate constant per unit weight of metal, k', was calculated from the data on Tables 1 and 4 and its logarithm was plotted against the logarithm of the corresponding particle diameter (Fig. 9). In order that interaction between surface and gas phase molecules takes place, the latter must be sufficiently close to the former. Thus, there is a distance from the surface which characterizes a critical collision volume, that includes all the molecules entering collisions with the underlying surface. Statistically, this distance must be equal to the molecular mean free path, λ. Consider a spherical particle of radius, r, enveloped by a spherical gas volume of radius λ (mean free path volume) (Fig. 10). The rate of gas–surface collision is proportional to this volume and, in particular, to the ratio, R, of this volume to surface area. It is shown below that whenever the particle size is much larger than the mean free path, λ, variations in metal particle size do not influence the ratio R and consequently, the specific surface reactivity. However, if the particle size is of the order of magnitude of λ or less, the ratio R decreases with increasing particle

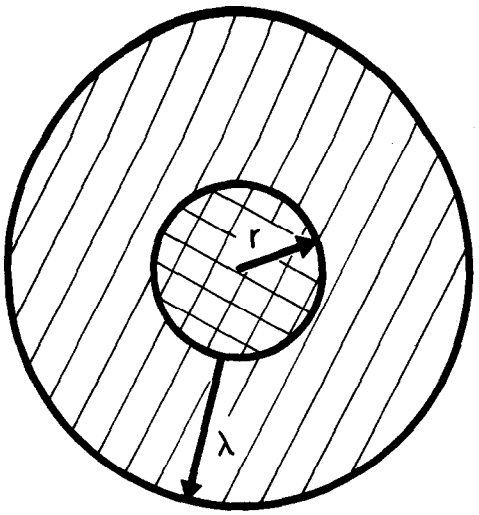

FIG. 10. Model for a spherical metal particle of radius, r, surrounded by a gas shell of thickness λ.

size and the specific surface reactivity is affected. This model, stresses the important role of the gas mean free path in relation to particle size, and it is physically consistent, since λ increases with temperature, and, consequently, the critical volume and the collision rate also increase.

The critical gas phase volume is (Fig. 10) $\frac{4}{3}\pi(3r^2\lambda + 3r\lambda^2 + \lambda^3)$, where r is the particle radius and the volume per unit surface area of the particle is:

$$R = \frac{1}{3}\left((3\lambda + 3\frac{\lambda^2}{r} + \frac{\lambda^3}{r^2}\right) = \lambda\left(1 + \frac{\lambda}{r} + \frac{1}{3}\left(\frac{\lambda}{r}\right)^2\right). \quad (9)$$

For a given set of experimental conditions λ = const. To find the effect of r upon R and thus upon the gas phase interaction, it is convenient to consider two limiting cases:

(i) $\lambda/r \ll 1$. This condition corresponds to a very large particle or flat surface ($r = \infty$). Since $(\lambda/r)^2 \ll \lambda/r \ll 1$, from Eq. (9) $R = \lambda$ = const and no surface effect is expected.

(ii) $\lambda/r \gg 1$. Since $(\lambda/r)^2 \gg \lambda/r \gg 1$ from Eq. (9) $R \cong \lambda(\lambda/r)^2$ or $R \propto r^{-2}$. In this case, surface effects will be present. Thus, whenever particle size increases from λ to a very large value, R decreases from 3λ to λ.

The total metal surface area per unit weight of metal, S is $\propto (1/r)$. The reaction rate constant referred to unit weight of metal, k', should vary with λ as shown in Table 5.

TABLE 5
RELATION BETWEEN RATE CONSTANT PER UNIT WEIGHT OF METAL, k', METAL PARTICLE RADIUS, r, AND GAS MEAN FREE PATH λ

$\lambda \ll r$	$k' \propto r^{-1}$
$\lambda \gg r$	$k' \propto r^{-3}$
$\lambda \approx r$	$k' \propto r^{-2}$

At the experimental conditions employed (350°C, 50 Torr), $\lambda = 2800$ Å. The expected slopes of plots of log k' vs log d are compared with the experimental ones in Fig. 9. The bulk of the experimental results can be fitted to a line with slope —3, indicating that the specific surface area of Au did have considerable effect on the rate of reaction (1). This is an interesting result in view of the fact that in most previous studies on the dispersion effect, no influence of the specific surface area of the metal was detected, down to small particle diameter (~20 Å). Whether this is a result of the catalyst preparation method employed or of the oxygen transfer step investigated cannot be assessed readily. It is tempting to speculate upon the influence of the preparative conditions of the catalyst and of the surface structure and morphology of the support to yield an environment for the metal particle in the finished catalyst, where molecular encounters, molecule–molecule and molecule–surface, may freely take place and the influence of the molecular mean free path relative to particle size, as suggested in this study, may be easily detected.

Clearly, the model proposed is a crude approximation to the actual physical conditions present at the metal particle imbedded into the matrix since it assumes that the conditions are similar for all the particles. Furthermore, no overlapping among critical volumes has been considered. This may be valid for low metal concentration and not too high metal dispersion. At sufficiently high dispersion, however, the number of metal particles may increase to the

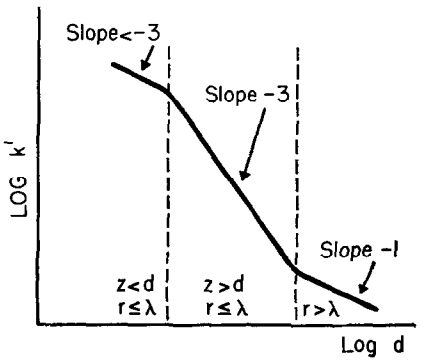

FIG. 11. Influence of intraparticle distance, z, particle diameter d and gas mean free path, λ, on surface reactivity, k', per unit metal weight.

extent that more than one particle will share part of the same critical volume. Where this effect sets in the specific collision rate will be reduced and, consequently, the catalytic activity will not increase as expected. The effect is schematically represented in Fig. 11.

Controlling Reaction Step

It is interesting to note that the value of the recorded activation energy, ~25 kcal mole^{-1} is less than half than that obtained on Au films at high temperature (~1000°C) (*5*). This value excludes the possibility of rate control by a reaction step taking place in the adsorbed phase [reaction step (b)]. A sequence of adsorption–desorption steps should include the controlling stage of reaction (1), namely:

$$*CO_2(g) \rightarrow *CO_2(s), \quad \text{(a)}$$
$$*CO_2(s) \rightarrow *CO(s) + O(s), \quad \text{(b)}$$
$$*CO(s) \rightarrow *CO(g). \quad \text{(c)}$$

Semiempirical calculations of the pre-exponential factor, k_0, by absolute rate theory for the cases of mobile and immobile adsorption were employed to indicate the role of the reaction steps (a) and (c). For Au at 350°C, the values per unit metal area are:

$$k_0,i = 3.4 \times 10^{-5} \text{ [mole cm}^{-2} \text{ sec}^{-1} \text{ atm}^{-1}\text{]},$$
$$k_0,m = 2.8 \times 10^{-2} \text{ [mole cm}^{-2} \text{ sec}^{-1} \text{ atm}^{-1}\text{]}.$$

For Pt at 450°C,

$$k_0,i = 2.34 \times 10^{-7} \text{ [mole cm}^{-2} \text{ sec}^{-1} \text{ atm}^{-1}\text{]}$$
$$k_0,m = 0.25 \text{ [mole cm}^{-2} \text{ sec}^{-1} \text{ atm}^{-1}\text{]}.$$

The experimental results are reported in Table 6.

TABLE 6

EXPERIMENTAL VALUES OF THE PRE-EXPONENTIAL FACTOR, k, PER UNIT OF METAL SURFACE, FOR REACTION (1) CATALYZED BY Au–MgO, (350°C) AND Pt–Al_2O_3 (405°C)

Metal	Wt %	$k_0 \times 10^2$ (mole cm^{-2}sec^{-1} atm^{-1})
Au	0.3	5.1
Au	0.7	3.1
Au	2.0	21
Au	5.0	1.5
Pt	1.0	150

Comparison between the experimental and the calculated value shows that agreement within one order of magnitude is obtained with the model of mobile activated complex. The sample containing 2% Au is off by about one order of magnitude.

CONCLUSIONS

The onset of catalytic activity for oxygen transfer at Au surfaces at ~350°C is a direct result of the enhancement of the Au–oxygen interaction by the dispersion of the metal on a rather inert support. Since below ~0.30 Tm direct intraparticle sintering does not take place readily, a high thermally stable Au dispersion is obtained by low temperature chemical reduction of the Au salt in the presence of the support. This preparation method permits the study of supported catalysts at similar degree of dispersion but different extent of metal area per gram of catalyst (metal plus support). In this fashion, effects dependent upon the extent of metal-to-metal particle proximity may be brought to light and their influence upon catalyst activity and selectivity investigated. The results obtained underline the paramount influence of the preparative method upon the genesis of the catalyst, and the critical role, indeed vital in the present study, of the support. Paradoxically it appears that MgO is the only successful support among those tested because

of its chemical inertness and relative low surface area. Possibly, these qualities permit the formation at low temperatures and the stabilization at higher temperatures of metal particles of small size and narrow size distribution.

Metal sites are the reactive surface centers for Au, Ru, and Pt for the oxygen transfer step investigated. In the case of Pt, however, a reactivity inversion is observed at higher temperatures and oxygen partial pressures. For Au, a decrease in particle size brings an increase in the surface affinity for oxygen. Since the oxidation depth of a molecule and the extent of selective oxidation behavior of a catalyst are dependent upon an optimum content of adsorbed oxygen with a characteristic heat of adsorption, this result indicates clearly that by optimization of particle diameters selective behavior in catalytic oxidations should be achieved. In addition to influencing the thermodynamics of the Au surface–oxygen interaction, the degree of dispersion of the metal does introduce kinetic effects in the rate of the oxygen transfer step. It is plausible to trace the origin of this influence upon the relative values of the gas mean free path and particle diameter. The presence or absence of the effect should be dependent upon physical factors in the juxtaposition of metal particle and support, and, should require a rather "free" metal particle on the support.

Finally, a mobile activated adsorption complex is in best agreement with semiempirical calculations of the absolute transfer rate. This is also consistent with the expectation of a relatively low adsorption heat of oxygen on Au.

In sum, the emerging picture of the active supported Au catalyst consists of small, spherical Au particles, formed in the presence, but independently of, MgO, rather loosely held at the MgO surface, yet thermally stable up to at least ~0.3 Tm. Upon this matrix, the particles are most exposed to gas phase collisions, and molecular encounters with the particle surface are statistically subjected to the molecular mean free path and its relation to particle diameter.

Acknowledgment

This work was supported by Grant GK-2013 from the National Science Foundation. This support is gratefully acknowledged.

References

1. Trapnell, B. M. W., *Proc. Royal Soc. Ser., A* **218,** 566 (1963); Bond, G. C., "Catalysis by Metals," p. 66, Academic Press, London/New York, 1962; Carpenter, L. D., Clark, D. E., Main, W. N., and Dickson, T., *Trans. Faraday Soc.* **55,** 1924 (1959); Clark, D., Dickson, T., and Main, W. N., *J. Phys. Chem.* **65,** 1470 (1961); Plumb, R. C., and Thakkar, N., *J. Phys. Chem.* **69,** 439 (1965).
2. Ford, R. R., and Pritchard, J., *Chem. Commun.* **1968,** 362.
3. Murgulescu, I. G., and Vass, M. I., *Rev. Roum. Chim.* **13,** 373, (1968).
4. Grabke, H. J., *Proc. Int. Congr. Catal., 3rd, 1964,* Vol. II, p. 928 (1965); *Ber. Bunsenges. Phys. Chem.* **69,** 48 (1965); Cha, D. Y., and Parravano, G., *J. Catal.* **11,** 228, (1968).
5. Grabke, H. J., *Ber. Bunsenges. Phys. Chem.* **71,** 1067, (1967).
6. Klug, H. P., and Alexander, L. E., "*X-Ray Diffraction Procedures,*" Chap. 9. Wiley, New York, 1954.
7. Delgass, W. N., Boudart, M., and Parravano, G., *J. Phys. Chem.* **72,** 3563, (1968).
8. Cha, D. Y., Ph.D. thesis, University of Michigan, 1968.